European Journal of Control (2008)6:1–15

DOI:10.3166/EJC.14.1–15

European Journal of Control

Hybrid Model Predictive Control of a Solar Air Conditioning Plant

P. Menchinelli* and A. Bemporad**

Department of Information Engineering, University of Siena, Italy

This paper describes the development and experimental validation of a multi-layer hybrid controller for optimizing energy management in a solar air conditioning plant. The hybrid nature of the process is due to its multi-mode structure: the refrigeration circuit can be fed by flat solar collectors, a storage system, by an auxiliary gas heater, or by a combination of them. The selection of the operating mode is obtained by switching electrovalves, pumps, and three-way mixing valves. The proposed multi-layer hybrid controller consists of a high-level supervisor that decides on-line the optimal operating mode through a hybrid model predictive control strategy, a static lower-level controller defining proper set-points for the chosen mode, and existing standard low-level controllers that ensure robust tracking of such set-points. The overall controller was designed in Matlab/Simulink using the Hybrid Toolbox, and then tested experimentally a real process, showing the effectiveness of the approach.

Keywords: Hybrid control systems, model predictive control, solar plants, mixed-integer programming

1. Introduction

The use of solar energy in air conditioning systems is one of the most appropriate ways of exploiting renewable energy sources, as solar heating power and user's cooling demand are synchronized in time. The use of storage systems and the associated thermal losses are henceforth minimized. In spite of this, solar refrigeration has not yet sufficiently exploited because of difficulties of implementation and hardware costs, which currently prevent the employment of solar refrigeration in small private houses. Nonetheless solar refrigeration is often a satisfactory solution in large buildings (i.e., public or work places), particularly in southern European countries where solar radiation is higher and at the same time energy consumption is larger in the summer than in the winter, mainly due to the massive use of conventional air conditioners.

Many techniques are available for producing refrigeration from solar energy [14]. One of the most successful is achieved by means of an absorption refrigerator that produces chilled water when hot water is injected into its generator. Because the energy needed to heat the water is provided by the sun, this kind of air conditioning systems reduces conventional energy consumption. However, to operate properly, an absorption refrigerator needs to meet specific operational conditions. We will discuss such operational conditions in Section 3.1.

As depicted in Fig. 1, besides an absorption cooler and solar collectors, a solar refrigeration plant also includes a storage system and an auxiliary gas-fired heater that occasionally compensates for lack of solar radiation, for instance in cloudy days. The configuration of the plant can be modified in real time by switching on/off electrovalves (binary manipulated variables), thus determining the set of currently active subsystems or, in other terms, the current *operating*

*E-mail: pmenchinelli@hotmail.it
**Correspondence to: A. Bemporad, E-mail: bemporad@dii.unisi.it

Received 11 April 2008; Accepted 17 September 2008
Recommended by E.F. Camacho, D.W. Clarke

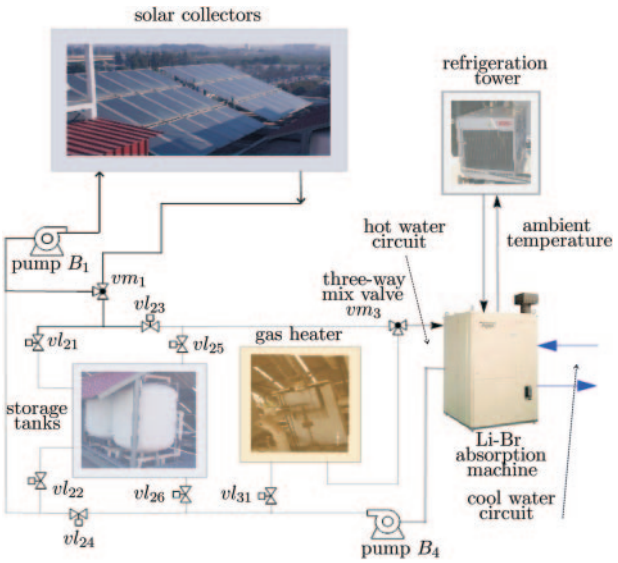

Fig. 1. Solar air conditioning plant (located in Seville, Spain)

mode, associated with each allowed combination of binary variables.

As the dynamics of the process strongly depends on both the operating mode and the value of other continuous variables, the system can be conveniently seen as a hybrid dynamical system [1, 4, 5]. Controlling hybrid dynamical systems is a particularly challenging task, due to the non-smooth nature of the dynamics. In the process at hand, the challenge is even further increased in a threefold way. First, the primary energy source, solar radiation, cannot be manipulated and must be considered as a measured disturbance, as in almost all thermal processes. Second, large disturbances on measured outputs and transport delays associated with water flows vary in time and depend on operating conditions. Third, the cooling demand is also variable, depending on the load applied to the refrigeration system. To complicate the control problem even further, the dynamics of the process are strongly nonlinear and linear identification tools fail to provide good models. While the literature on solar-powered plants is quite rich (see e.g., the contributions of [6] and [13]), very seldom the hybrid dynamical nature of the process is taken into account. Hybrid techniques for control of solar air-conditioning plants have appeared in [7, 20].

Recently, model predictive control (MPC) based on hybrid dynamical models has emerged as a very promising approach to handle switching linear dynamics, on/off inputs, logic states, as well as logic constraints on input and state variables [4]. The approach consists of modeling the open-loop hybrid process and existing operating constraints using the language HYSDEL [16] and then automatically transform the model into a set of linear equalities and inequalities involving both real and binary variables, denoted as the mixed logical dynamical (MLD) systems. As a consequence, the mathematical programming problem associated with the MPC controller can be written as a mixed-integer linear or quadratic programming (MILP/MIQP) problem, for which both commercial [11] and public domain [3, 12] solvers are available. The approach is versatile enough to allow one to embed several heuristic rules and penalties in the mixed-integer programming formulation when these can be modeled as mixed logical/linear constraints [10, 17, 18]. However, compared to pure rule-based approaches, here the control inputs are not decided by fixed rules, but rather chosen optimally with respect to a performance index among the feasible ones, depending on the current operating conditions.

Rather than modeling the complete system in MLD form and applying a monolithic hybrid MPC solution, in this paper we have adopted a hierarchical solution, where a hybrid MPC supervisor decides the current operating mode and low-level controllers ensure reference tracking and robustness. A monolithic hybrid MPC solution was indeed tested by the authors by modeling the whole system in piecewise affine form (switched linear difference equations, as suggested in [19]), but the resulting mixed-integer optimization problem was too complex to be solved within the available sampling period and not enough robust, due to excessive model/plant mismatch.

Although it provides a suboptimal solution, the hierachical approach described in this paper preserves

the basic hybrid structure of the problem and, as will be shown, provides a satisfactory closed-loop performance. The control problem is divided into two steps. First, the hybrid MPC supervisor provides the optimal operating mode for the next time step, based on an abstracted model described in MLD form through the HYSDEL Programming Language. The currently most suitable operating configuration is computed by solving a relatively small-size MIQP problem on line. Then, the current values for the continuous variables are computed according to the chosen operating mode by exploiting control maps derived from experimental results, and tracked by the lower level controllers.

The hierarchical hybrid MPC control structure introduced above has been implemented in Matlab/Simulink using the Hybrid Toolbox for Matlab [2] and the OPC Toolbox for Matlab [15] on a solar air conditioning process. The obtained experimental results are reported at the end of this paper.

2. Plant Description

The solar air conditioning plant considered in this paper is located at the Automation Department of the University of Seville, Spain. The plant was proposed as a benchmark problem for hybrid control approaches within the European Network of Excellence HYCON (http://www.ist-hycon.org). It consists of a surface of flat solar fields placed on top of the department building that supply heat to a Yazaki single-effect Li-Br absorption machine to carry out the cooling process. In addition, the plant is composed to two buffer storage tanks and an auxiliary gas-fired heater. The process is depicted in Fig. 1, its block schematic and system variables are shown in Fig. 2. The main components of the plant are described below:

Cooling system. This carries out the refrigeration process by means of a single-effect absorption machine with two separated circuits: a *generator* (with a high pressure) and an *evaporator* (almost under vacuum). During proper system operation, water heated in the plant flows into the generator, losing the necessary heat to bring the Li-Br water solution to the boiling point (75–100 °C). In the evaporator, vapor of refrigerant (H_2O) coming from the generator gets out condensed at a lower temperature, after having flowed through a laminar valve that decreases its enthalpy. The heat produced in the condenser (about 30 °C) is dissipated in the environment by a refrigeration tower. Then, in consequence of a very low pressure, the refrigerant evaporates at low temperatures (>6 °C), thus cooling the inlet water coming from the air conditioned circuit (typically 15–22 °C). The last step is absorption, in which vapor of refrigerant comes back in the concentrated solution and the cycle is ready to continue. Such a *continuous absorption* machine is internally composed of four parts: generator, condenser, evaporator, and absorber. Incorrect operation of anyone of these parts may cause a damage to the whole machinery. To tackle this issue, a built-in controller regulates a solution pump that keeps the correct solution concentration. A bypass at the entrance of the generator deviates the flow if the temperature of the

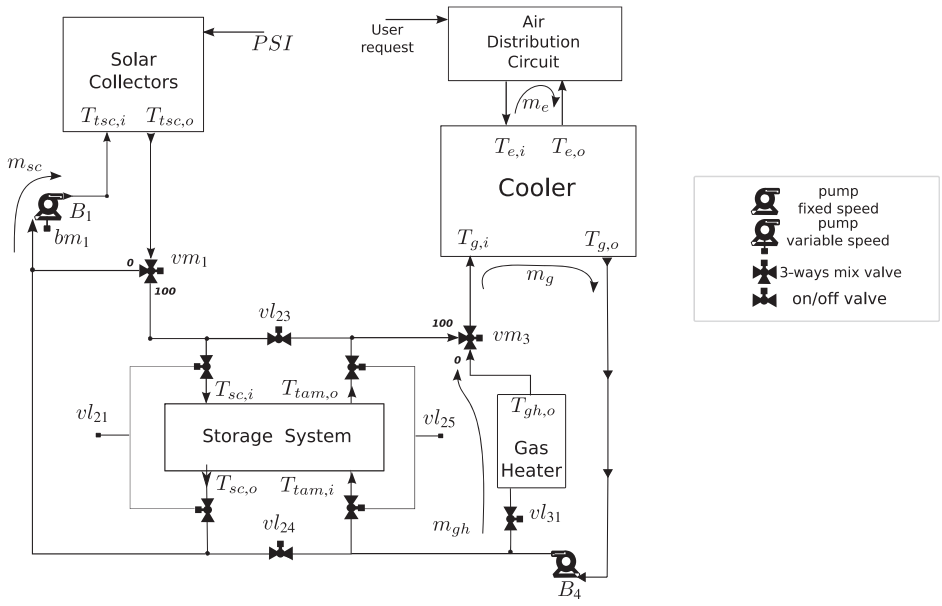

Fig. 2. Schematic of the solar air-conditioning plant

inlet water $T_{g,i}$ is below 75 °C. Despite this, having $T_{g,i} \geq 75$ °C does not ensure the correct operation of the absorber: during start-up, for example, $T_{g,i} \geq 85$ °C is needed to start the refrigeration process and, during normal operation, the lower bound can vary between 78 and 80 °C, depending on the flow in the generator (m_g) and on the internal concentration of Li-Br in the generator (that cannot be measured). For control purposes only two subparts of the cooler have been considered: generator and evaporator. The dynamics of the cooler has been neglected, as it is anyway impossible to avoid oscillations at the output of the evaporator ($T_{e,o}$) and to control exactly the temperature at the input of the generator ($T_{g,i}$). The goal becomes then to keep the cooler working properly.

Solar system. The solar system is composed of $151 m^2$ of flat collector surface, which can work in the range [60,100] °C and provide the main source of energy in the system. The output temperature $T_{sc,o}$ depends on the solar irradiation per surface unit (W/m^2), on the inlet temperature $T_{sc,i}$ and on the water mass flow m_{sc}, and on the external temperature of the environment. The flow m_{sc} is imposed by the pump $B1$. The signal $B1$ enables the pump and $bm1$ regulates its speed, thus driving the flow m_{sc}. The dependence of m_{sc} on $bm1$ is nonlinear and depends on the operating configuration [19]. A model for the solar collectors has been investigated by means of (i) differential equations that estimate the internal average temperature, computing the predicted value of the output by interpolating inlet and average temperatures of the equipment, and (ii) variable transport delays due to flows and heat capacity of the collectors. Having in mind only the control task, we neglect such a model here and only consider energy balances to predict steady-state behaviors. Solar radiation is measured by a sensor on top of the building hosting the process, near the collectors. Both instantaneous values and values averaged over a period of five minutes are employed for feedback.

Accumulation system. This is composed of two tanks of $2500l$ capacity working in parallel, having average temperatures $T_{tsc,o}$ and $T_{tam,o}$ that are measured separately in each tank. The water is stored in the tanks when the solar power is high and can be used when the solar radiation falls down (e.g., because of a temporary cloud). The absence of an inner mixer makes the temperature distribution rather stratified, because the hot water migrates to the upper level toward the absorption circuit. The estimate of the inner temperature of the tanks is therefore rather approximate, as only inlet and outlet manifold temperatures can be measured. Variables T_{tsc} refer to the accumulation circuit that links tanks to solar collectors, T_{tam} refer instead to the circuit connected to the absorption machine (cooler). The measurements of $T_{tsc,i}$, $T_{tsc,oh}$, and $T_{tam,i}$ are reliable only when significant flow pass through the respective manifolds. Measurements of $T_{tam,o}$ are instead rather reliable and are used in the control application design.

Auxiliary system. This is composed of a gas-fired heater with a nominal heating power of $47 kW$ that can be used as an auxiliary energy source to feed the chiller when solar fields output temperature is not enough. The existing heater has a built-in on/off controller which makes the output temperature rather oscillatory, avoiding damages due to thermal inertia. The oscillatory nature is given by a thermostat that turns off the burner when the output temperature $T_{gh,o}$ reaches 90 °C and re-activates the burner only when the temperature falls below 84 °C. It may frequently happen, however, that the output temperature in the off cycle falls under 80 °C if the inlet temperature is low. Further, due again to thermal inertia, it is not allowed to close valve vl_{31} when the output temperature is above 75 °C, and if the flow m_{gh} is less than $1500 l/h$ the burner is automatically turned off.

2.1. Notation

The variables of interest shown in the schematic of Fig. 2 are described in Table 1, along with the corresponding range of allowed values, and are classified as follows: manipulated variables (MV), measured disturbances (MD), and measured outputs (MO).

2.2. Operating Modes

The manipulated variables of the system are either discrete and real valued. Binary manipulated variables define the *operating mode* of the process, as described in Table 2. Note that only a subset of combinations of binary manipulated variables are admissible, according to the analysis of experimental data collected during proper operation of the equipment.

The different admissible operating modes are described below:

1. *M1. Recirculation*. All water flows through the solar collectors, whose internal temperature is increased.
2. *M2. Loading tanks*. The water in the solar collectors is accumulated inside the tanks.
3. *M3. Using solar collectors*. Water is heated in the solar collectors and flows to the cooler, feeding the refrigeration process.

Table 1. Variables of interest

Type	Name	Physical meaning	Value	Type
MV	bm_1	Pump B1 speed	$0 \div 100\%$	Continuous
MV	vm_3	3-Ways valve position	$0 \div 100\%$	Continuous
MV	vm_1	3-Ways valve position	{0,100}	Discrete
MV	B_4	Enable pump B4	{0,1}	Discrete
MV	B_1	Enable pump B1	{0,1}	Discrete
MV	vl_{31}	Electrovalve	{0,1}	Discrete
MV	vl_{21}	Electrovalve	{0,1}	Discrete
MV	vl_{23}	Electrovalve	{0,1}	Discrete
MV	vl_{25}	Electrovalve	{0,1}	Discrete
MD	PSI	Solar radiation power	W	
MD	m_e	Evaporator flow	l/h	
MO	m_{sc}	Solar collectors flow	l/h	
MO	m_{gh}	Gas heater flow	l/h	
MO	m_g	Generator flow	l/h	
MO	$T_{g,i}$	Generator inlet temperature	°C	
MO	$T_{g,o}$	Generator outlet temperature	°C	
MO	$T_{e,o}$	Evaporator outlet temperature	°C	
MO	$T_{sc,o}$	Solar fields outlet temperature	°C	
MO	$T_{gh,o}$	Gas heater outlet temperature	°C	
MO	$T_{tam,o}$	Tanks outlet temperature (to cooler)	°C	
MO	$T_{tsc,o}$	Tanks outlet temperature (to solar fields)	°C	
MO	$T_{tsc,i}$	Tanks inlet temperature (from solar fields)	°C	

Table 2. Operating modes of the solar refrigeration plant

Mode	Cooler	vl_{21}	vl_{23}	vl_{25}	vl_{31}	B_4	B_1	vm_1
M1. Recirculation	Off	0	0	0	0	0	1	0
M2. Loading tanks	Off	1	0	0	0	0	1	100
M3. Use solar ($m_{gh} < 1500\,l/h$)	On	0	1	0	1	1	1	100
M4. Use solar + gas ($m_{gh} > 1500\,l/h$)	On	0	1	0	1	1	1	100
M5. Use gas only	On	0	0	0	1	1	0	0
M6. Use tanks only	On	0	0	1	0	1	1	0
M7. Use tanks + gas	On	0	0	1	1	1	1	0
M8. Load tanks + gas	On	1	0	0	1	1	1	100
M9. Recirculation + gas	On	0	0	0	1	1	1	0

4. *M4. Using solar collectors with gas heater on*. The water coming from the solar collectors is mixed with the water heated in the gas burner. The flow distribution, and hence the gas consumption, depends on the mix valve vm_3.
5. *M5. Using gas heater only*. In this mode the cooler is supplied only by the gas heater. The solar collectors are turned off by setting pump velocity $bm_1 = 0$.
6. *M6. Using the tanks*. The cooler is supplied by water previously stored in tanks, meanwhile the water in the solar collectors is recirculated to increase their output temperature.
7. *M7. Using the tanks with gas heater on*. Water coming from the tanks is mixed with water from the gas heater to supply the generator circuit of the cooler. Water in solar collectors is recirculated.
8. *M8. Loading the tanks while using the gas heater*. The cooler is supplied only by the heater, while the tanks are recharged with the water coming from the solar collectors.
9. *M9. Recirculating while using the gas heater*. The cooler is supplied only by burning gas, while water in the solar collectors is recirculated to increase the temperature.

2.3. Identification of Thermal Losses

The losses due to heat transportation between the subsystems of the plant are described in Table 3. These were estimated from experimental data using standard linear regression. In the absence of direct links between two different piece of equipment the entry of the table is empty.

Internal losses of the equipments have been neglected. The losses that most affect system

Table 3. Thermal losses between equipments

From/To	Absorption machine	Solar collectors	Storage tanks	Gas heater
Absorption machine	-	$L_{am,sc} \approx 1\,^{\circ}\mathrm{C}$	$L_{am,t} \approx 1^{\circ}C$	$L_{am,gh} \approx 1^{\circ}C$
Solar collectors	$L_{sc,am} = f(vl_{23})$	-	$L_{sc,t} \approx 0.5^{\circ}C$	-
Storage tanks	$L_{t,am} \approx 1\,^{\circ}\mathrm{C}$	$L_{t,sc} \approx 0.2\,^{\circ}\mathrm{C}$	-	-
Gas heater	$L_{gh,am} \approx 1\,^{\circ}\mathrm{C}$	-	-	-

operation are $L_{sc,am}$, $L_{t,am}$ and $L_{gh,am}$, as they lead to relevant drops in controlled temperatures. Thermal loss $L_{sc,t}$ is relevant in the accumulation mode M2 and it must be taken into account when computing the minimum temperature of the collectors. Other losses are not relevant to our control purpose since they do not have a direct impact on the controlled variables. Thermal losses $L_{t,am}$ and $L_{gh,am}$ are rather constant and are replaced by their maximum value, which is estimated as $1\,^{\circ}\mathrm{C}$ in the worst case (it is often smaller). Thermal loss $L_{sc,am}$ instead can vary between $2 \div 7\,^{\circ}\mathrm{C}$. Given this relatively large range, rather than replacing the loss with a static constant worst-case estimate, $L_{sc,am}$ is estimated dynamically as the output of a first order linear system with time constant equal to 150 seconds. The estimation is performed by considering two different situations, depending on the use of the solar collectors (indicated by the valve vl_{23}). When solar collectors are not used ($vl_{23} = 0$) the loss function increases up to the maximum value of $7\,^{\circ}\mathrm{C}$; when the valve is opened $L_{sc,am}$ converges to the minimum value of $2\,^{\circ}\mathrm{C}$. Note that the loss functions depend also on the temperatures of sources and pipelines, which are considered constant in the operating region used in the experiments.

3. Control Problem and Proposed Strategy

The control objectives (in order of importance) are summarized below:

- The temperature of cooled water must track a given reference set-point;
- Gas consumption (= use of gas heater) must be minimized;
- Heat stored in the tanks must be maximized;

The goals must be achieved by manoeuvering the following manipulated variables:

- *Binary inputs*: the position of electrovalves vl_{21}, vl_{23}, vl_{25}, vl_{22}, vl_{24}, vl_{26}, vl_{31}, of the three-way valve vm_1, and the status of the on/off pump B_4;
- *Continuous inputs*: the velocity bm_1 of pump B_1, the position of the three-way mix valve vm_3.

In this paper we hierarchically organize the control setup in two layers: the upper layer decides the current value of the binary inputs and consequently the current operating mode, the lower layer decides the current value of the continuous inputs through static maps that depend on the operating mode selected for the next time step and process values at the current time. The main control objective is to supply chilled water (T_{eo}) to the air distribution system, according to the requested temperature (assumed here to be $15\,^{\circ}\mathrm{C}$), while minimizing gas consumption and, if possible, increasing the energy stored in the tanks at the end of the day. From experimental observations it turns out that, in order to properly feed the absorption machine, the inlet temperature of generator (T_{gi}) should lie in the range $[78.5 \div 100]\,^{\circ}\mathrm{C}$. The energy needed for the cooling process can be derived from solar flat collectors or, as alternative choices, from either the storage system or the auxiliary system.

The nine operating modes shown in Table 2 were selected to represent all possible useful configurations to achieve the control goals. The choice of the operating mode (through the corresponding combination of binary inputs) is performed by a hybrid MPC supervisor based on an abstract hybrid model of the process.

The overall control strategy consists of a hierarchical hybrid controller, as depicted in Fig. 3, where continuous and binary inputs are controlled separately. The sampling time of the whole controller is $T_S = 10s$. In the next sections, after describing the way the cooler should operate correctly, we define both control layers in detail.

3.1. Proper Operation of the Cooling System

The cooler realizes an absorption cycle quite similar to the steam compression cycle of conventional conditioners, except that steam is not mechanically forced, but comes from boiling the refrigerant fluid (water in this case). The water is firstly separated from the

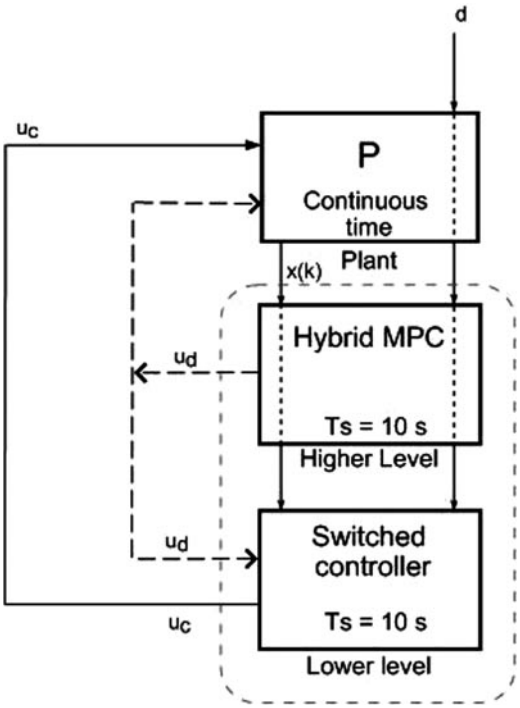

Fig. 3. Hierarchical control setup

solution in the generator by supplying its latency heat, and then the solution is renewed by absorbing the condensed refrigerant at low pressure. This cycle is repeated continuously.

To produce refrigeration this machine needs heat to bring the solution to the boiling point, supplied by the equipment described in the previous sections, and can vary depending on both the amount of heat extracted from cold source and the concentration of solution in the generator. The criterion adopted to estimate the status of the absorber is based on the analysis of the heat absorbed by the generator (needed to bring the refrigerant to the boiling point). Basically, when the mean power absorbed is positive the machine is working properly and is in a steady-state condition.

The average inlet heat $\overline{(T_{g,i} - T_{g,o})m_g}$ is considered instead of the instantaneous power in order to improve robustness properties, thanks to the filtering action on disturbances. The lower bound $T_{g,iLB}(k)$ on $T_{g,i}(k)$ was determined experimentally as follows:

$$T_{g,iLB}(k) = \begin{cases} 78.5\,^{\circ}\mathrm{C} & \text{in proper operation} \\ 80\,^{\circ}\mathrm{C} & \text{in proper operation, with low } m_g \\ 85\,^{\circ}\mathrm{C} & \text{otherwise} \end{cases} \tag{1}$$

where $k = 0, 1, \ldots$ is the sampling step. The value of $T_{g,iLB}(k)$ is then used by the controller in order to choose the next operating mode and set the continuous variables. In addition, when the generator flow $m_g(k)$ is low, typically while using the gas heater, the lower bound temperature for $T_{g,i}(k)$ is increased to 80 °C for proper operation, in order to give stability and better performances of the cooler while minimizing the flow, and hence the heat loss by the gas heater to both the environment and the cooler.

Table 4. Continuous inputs: pump velocity bm_1 and 3-way mix-valve position vm_3

	M1	M2	M3	M41	M40	M5	M6	M7	M8	M9
bm_1	50	100	30	70	10	not used	50	50	50	50
vm_3	50	50	95	70	91.5	not used	95	85	90	90

3.2. Switched Static Controller (Continuous Inputs)

Continuous inputs vm_3 and bm_1 are manipulated through switched static maps based on the mode selected by the high-level controller described below in Section 3.3.

The default values for the continuous inputs with respect to the operating mode are shown in Table 4, where mode M4 is divided into two main submodes that reflect different settings for continuous inputs: M40 is the submode with the minimum flow in the gas heater (while keeping burner on) and is used when output temperature of the heater is low, while M41 is used when $T_{gh,o}$ have reached its nominal value.

During recirculation an intermediate speed for pump B1 is selected. This takes into account that, if m_{sc} is too small, solar collectors dissipate more energy to the environment. On the other hand, when m_{sc} is too large, $T_{sc,o}$ grows less. During accumulation the speed of pump B1 has been set to its maximum value in order to maximize the energy stored in the tanks. In general, the proper choice of vm_3 can provide a minimization of gas consumption and of the response of the gas heater and of the evaporator (the settling time of the output temperature). The valve configuration used in mode M3 allows working with the gas heater valve vl_{31} open without any gas consumption, as the burner stops working if the flow is very small.

3.3. High-level Supervisor (Binary Inputs)

The objective of the hybrid supervisor is to determine the best operating mode M_i^* for the next time step by manipulating the binary inputs of the plant. The selection criterion is based on the minimization of a mode-dependent piecewise-affine heuristic cost function,

dependent on the energy balance between subsystems, subject to mixed linear and logical constraints.

The latter encode several heuristics about what the controller *must* do (hard constraints) and what it *should* do (soft constraints). Contrarily to strategies where the mode is selected according to a set of certain operating rules, here the controller has more degrees of freedom in choosing the current operating mode, that can be therefore be chosen optimally among all possibile modes that satisfy the current operating conditions of the system by solving a mixed-integer optimization problem on line.

3.3.1. Hard Constraints

To ensure that the optimal mode selection is unique the following exclusive-or condition

$$\sum_{i\in\{1,\cdots,10\}} M_i(k) = 1 \tag{2}$$

is imposed, where $M_i(k) \in \{0,1\}, \forall i = 1,\ldots,10$, is 1 if and only if the system is in mode Mi at time k, $k = 0,1,\ldots$.

The set of operating modes is divided into two subsets on the basis of the cooling demand (evaporator flow), as described in Table 5. Partitioning the available modes in this way allows one to define a heuristic rule that helps the high-level controller out in taking an optimal decision (and that, in fact, reduces the computational load associated with the controller). By interpreting refrigeration requests by the user through the amount of evaporator flow, the heuristic rule is modeled as follows:

$$\begin{aligned}
&[m_e(k) < 3000] \;\rightarrow\; [M_1(k) = 1] \vee [M_2(k) = 1] \\
&[m_e(k) \geq 3000] \;\rightarrow \bigvee_{i=3}^{10} [M_i(k) = 1]
\end{aligned} \tag{3}$$

Keeping into account (2), the rule defined by (3) can be interpreted as follows:

- No request of refrigeration by the user (evaporator flow $m_e < 3000$ l/h): the controller can switch only between modes M1 and M2, alternating between recirculation in the collectors and tank loading.

Table 5. Subsets of operating modes defined by cooling demand

Evaporator flow (l/h)	Operation mode subset	Subset
< 3000	M1,M2	NOT COOLING
≥ 3000	M3,M4,M5,M6, M7,M8,M9,M10	COOLING

- Cooling request by the user (evaporator flow $m_e \geq 3000$ l/h): the absorption machine must be activated and the choice falls over the modes of the remaining modes M3–M10.

The management of storage tanks imposes further constraints. When the absorption machine is not working, there must be no gas consumption. The costs associated with modes where gas is not used are fixed costs, where accumulation is preferred to recirculation. However, the choice between M2 and M1 must take into account hard constraints that avoid the use of accumulation (regulated by the valve vl_{21}) when this is not suitable:

$$[T_{TSCI}(k) \leq T_{LBACC}(k)] \;\rightarrow\; [vl_{21}(k) = 0] \tag{4a}$$

where

$$\begin{aligned}
&T_{TSCI}(k) \\
&= \begin{cases} T_{tsci}(k) & \text{if } [vl_{21}(k-1) = 1] \\ T_{sco}(k) - L_{sc,t} & \text{otherwise} \end{cases} \\
&T_{LBACC}(k) \\
&= \begin{cases} T_{tsco}(k) & \text{if } m_e(k) < 3000 l/h \\ \max\{T_{tsco}(k), T_{tamo}(k)\} & \text{otherwise} \end{cases}
\end{aligned} \tag{4b}$$

where $vl_{21}(k-1) = 1$ indicates that the system was in accumulation mode (M2 or M8) at the previous time step $k-1$, $m_e(k)$ is the evaporator flow, $T_{tsci}(k)$ is the tank inlet pipe linked to the solar collectors, $T_{sco}(k)$ is the output of solar collectors, $T_{tsco}(k)$ the tank outlet pipes to the solar collectors, $T_{tamo}(k)$ is the tank output to the absorption machine, $T_{gi,REF}$ is the actual reference for the inlet temperature of the generator, $L_{sc,t}$ is the transport loss (see Table 3). Note that the constraint in (4) regulates the use of accumulation also when the cooling action is active.

The basic condition to avoid energy losses in tanks imposes that the inlet temperature of tanks T_{tsci} must never be less than the tank outlet temperature T_{tsco}. According to Eq. (4) the condition for exiting from accumulation modes can vary, depending on the previous operating mode: if the previous mode was M2 or M8 then the tank inlet temperature will be measured directly at the input of the tanks, otherwise it will be estimated from the output temperature of the solar collectors. The measurement of T_{tsci}, in fact, is not reliable when tanks are closed since the sensor is placed externally and its measure falls suddenly along with the temperature of the pipes. With this kind of control the system will alternate modes M1 and M2 until T_{tsci} warms up, thus minimizing losses linked to cold water in the pipes.

The following hard constraint prevents the use of mode M3 when inappropriate:

$$[T_{sco}(k) - L_{SC,AM} \leq \widehat{T}_{gi,sc}(k) + \Delta_{SC,M3}(k)] \rightarrow [M_3(k) = 0] \quad (5a)$$

where

$$\widehat{T}_{gi,sc} = \begin{cases} a_{40} T_{GI,ref} - (a_{40} - 1)(\widehat{T}_{gwo}(k) - L_{GH,AM}) & \text{if } [\widehat{T}_{gwo}(k) \leq 81.5] \wedge [vl_{31}(k) = 1] \\ T_{GI,ref} & \text{otherwise} \end{cases} \quad (5b)$$

and

$$\Delta_{SC,M3}(k) = \begin{cases} \delta_1 & \text{if } M_3(k-1) = 1 \\ \delta_2 & \text{otherwise} \end{cases} \quad (5c)$$

The value of coefficient a_{40} is reported in Appendix A in Table 7. In (5) $\widehat{T}_{gi,sc}$ represents the minimum value of T_{sco} needed to obtain $T_{gi} = T_{GI,ref}$, without considering transport losses $L_{SC,AM}$. Coefficient a_{40} depend on the flow distribution through the devices, estimated for the "emergency' configuration M4 as defined in the previous section. The temperature of the gas heater $\widehat{T}_{gwo}$ is estimated by keeping into account the state of the burner: when the burner is off, is estimated to be equal to its minimum value 81.5 °C, otherwise is equal to its measured value. Valve vl_{31} enables flow in the gas heater. If the valve is closed ($vl_{31} = 0$) the contribute of the gas heater is neglected and the lower bound for T_{sco} becomes equal to $T_{GI,ref}$. Buffer values $\Delta_{SC,M3}$ are reported in Appendix A, Table 6.

By computing the worst-case minimum value for $T_{sco}(k)$ at each time step k (corresponding to a sudden drop of solar irradiation), robustness against disturbances on the input of the generator is ensured with almost no added costs in gas consumption.

The controller can switch to mode M3 independently on the valve position vl_{31}, which depends instead on the actual temperature of T_{gwo}. The actual value of the gas heater valve is then adjusted from the lower level controller (the valve can be closed only if T_{gwo} is lower than 75 °C).

The high-level controller works always with a margin δ_1 (active only when leaving mode M3) on $T_{GI,ref}$ that permits safe activation of the gas heater in mix mode also when T_{gwo} is too low to directly activate the cooler.

When the cooler is fed with water coming only from the tanks (M6) the same considerations made for M4 hold. In fact, $\widehat{T}_{gi,tt}$ is derived similarly to $\widehat{T}_{gi,sc}$, with different coefficients. In this case, mode M7 is considered as an emergency solution. The execution of mode M6 is instead affected by the following constraint:

$$[T_{tamo}(k) - L_{T,AM}(k) \leq \widehat{T}_{gi,tt}(k) + \Delta_{TT,M6}(k)] \rightarrow [M_6(k) = 0] \quad (6a)$$

where

$$\widehat{T}_{gi,tt}(k) = \begin{cases} a_{70} T_{GI,ref} - (a_{70} - 1)(\widehat{T}_{gwo}(k) - L_{GH,AM}(k)) & \text{if } [\widehat{T}_{gwo}(k) \leq 81.5] \wedge [vl_{31}(k) = 1] \\ T_{GI,ref} & \text{otherwise} \end{cases} \quad (6b)$$

and

$$\Delta_{TT,M6}(k) = \begin{cases} 0 & \text{if } \widehat{T}_{gi,M4}(k) > T_{GI,ref} + \delta_1 \\ \delta_5 & \text{otherwise} \end{cases} \quad (6c)$$

with

$$\widehat{T}_{gi,M4}(k) = \frac{1}{a_{40}}(T_{sco}(k) - L_{scam}(k)) + \frac{a_{40} - 1}{a_{40}}(\widehat{T}_{gwo}(k) - L_{gham}(k)) \quad (6d)$$

The buffer $\Delta_{TT,M6}(k)$ changes according to the temperature $T_{sco}(k)$: if the temperature of the collectors is greater than the reference value, then it is not necessary a buffer, as it is possible to switch to M4 if the temperature of the tanks T_{tamo} falls suddenly; otherwise a positive buffer δ_5 is needed.

Table 6. Thresholds values

$\Delta_{SC,M3}$		$\Delta_{SC,M4}$		$\Delta_{TT,M6}$
δ_1	δ_2	δ_3	δ_4	δ_5
1.5	5	0	2.5	1.5

3.3.2. Soft Constraints

The constraints applied on mode M4 are quite similar to those on M3 but are treated as soft constraints:

$$[T_{sco}(k) - L_{scam}(k) \leq \widehat{T}_{gi,sc}(k) + \Delta_{SC,M4}(k)] \rightarrow [M_4(k) = 0] \vee [\gamma_4(k) = 1] \quad (7a)$$

where $\gamma_4(k) \in \{0,1\}$ is a *binary slack* variable that allows the condition $M_4 = 0$ to be violated, and

$$\widehat{T}_{gi,sc}(k) = \begin{cases} a_{40}T_{GI,ref} - (a_{40}-1)(\widehat{T}_{gwo}(k) - L_{gham}(k)) & \text{if } \widehat{T}_{gwo}(k) \le 81.5 \\ T_{GI,ref} & \text{otherwise} \end{cases} \tag{7b}$$

$$\Delta_{SC,M4}(k) = \begin{cases} \delta_3 & \text{if } vl_{23}(k-1) = 1 \\ \delta_4 & \text{otherwise} \end{cases} \tag{7c}$$

The main changes with respect to (5) are the different buffers of activation and deactivation (δ_3, δ_4) and the absence of variable vl_{31}, which is always 1 in mode M4. The values of buffer $\Delta_{SC,M4}$ are reported in Appendix A, Table 6.

The soft constraints preventing the use of mode M7 are defined as

$$[T_{tamo}(k) - L_{tam}(k) \;\le\; \widehat{T}_{gi,tt2}(k)] \;\rightarrow\; [M_7(k) = 0] \vee [\gamma_7(k) = 1] \tag{8a}$$

where $\gamma_7(k) \in \{0,1\}$ is the binary slack variable associated with mode M7 and

$$\widehat{T}_{gi,tt2}(k) = \begin{cases} a_{70}T_{GI,ref} - (a_{70}-1)(\widehat{T}_{gwo}(k) - L_{gham}(k)) & \text{if } \widehat{T}_{gwo}(k) \le 81.5 \\ a_{71}T_{GI,ref} - (a_{71}-1)(\widehat{T}_{gwo}(k) - L_{gham}(k)) & \text{otherwise} \end{cases} \tag{8b}$$

Note that the constraints in (8) are quite different with respect to the constraints in (6) on M6, as a submode has been introduced for M7 with high flow in the gas heater, in order to increase the use of the tanks. Coefficient a_{71} is calculated for this submode and is reported in Appendix A in Table 7. In this case the use of buffers is not required since the aim is to use the tanks as long as possible.

Finally, the use of gas heater only should be avoided if its output temperature is below 81.5 °C[1]:

$$[\widehat{T}_{gwo}(k) \le 81.5] \;\rightarrow\; [M_8(k) = 0 \wedge M_9(k) = 0] \vee [\gamma_{89} = 1] \tag{9}$$

The further condition

$$\gamma_4(k) + \gamma_7(k) + \gamma_{89}(k) \le 1 \tag{10}$$

imposes that at most one of the above constraints can be actually softened. In critical situations like the initialization of the system, it is possible to relax one of the above constraints. In such a case the goal is to choose the subsystem that supplies the higher temperature at the entrance of the generator. To achieve this, T_{gi} is estimated for all the devices, considering all the environmental losses associated with transportation.

3.3.3. Heuristic Cost Function

As mentioned earlier, a mean value is considered for the solar power *PSI*; this value is used to calculate the cost of each source of energy (solar, tanks and auxiliary). The heuristic cost function keeps into account the energy balance of the system, giving thus preference to the use of solar collectors only if the mean inlet solar power minus the transport losses can balance the energy consumption of the cooler. From experimental investigation on the plant, it was observed that energy consumption of the cooler is rather constant.

The cost function $C(k)$ to be minimized is defined as follows

$$C(k) = \sum_{i=1}^{9} C_i(k) + \rho(\gamma_4(k) + \gamma_7(k) + \gamma_{89}(k)) \tag{11a}$$

where

$$C_i(k) = \begin{cases} W_i & \text{if } M_i(k) = 1 \\ 0 & \text{otherwise} \end{cases} \tag{11b}$$

Table 7. Coefficients used in Equations (5a), (6), (7), (8)

a_{40}	1.4800
a_{41}	1.5818
a_{70}	1.3129
a_{71}	1.8015

[1]Note that $81.5 - L_{GH,AM} = 80.5 < 78.5$: when using the gas heater only, due to a lower generator flow, the minimum temperature for T_{gi} becomes higher.

and constants W_i are defined as

$$W_i = \begin{cases} P_i - \Delta E_s & \text{if } i \in \{1,2,3,4,8,9\} \\ P_i & \text{if } i \in \{6,7\} \end{cases} \quad (11c)$$

In (11) W_i is the penalty associated with mode Mi, ΔEs is a function of the current solar irradiation, and P_i is a fixed cost associated with the use of mode Mi that depends on the incentives in using solar irradiation. The penalty ρ is chosen high enough to force the binary slack variables γ_4, γ_7, γ_{89} to zero in nominal conditions ($\rho = 1000$ in the control setup described in Section 4).

Qualitatively, the heuristic cost function takes into account the following preferences:

- Solar collectors are preferred only when *PSI* reaches the minimum value needed to perform the task. A little buffer is considered in order to give more robustness to disturbances such as little clouds. Solar collectors, in fact, seem to have an inner thermal buffer, as observed in response to small irradiation disturbances.
- The solely use of gas heater (M8/M9) is performed only when no other device is suitable. However, if *PSI* cannot balance the minimum estimated energy needed by the cooler plus the transport losses, then the auxiliary source is preferred to the solar collectors (M3/M4), since T_{sco} will suddenly fall.
- Tanks are always preferred as energy source (M6/M7) against the gas heater, if their temperature is enough to feed the cooler.

When the cooler is working, the priority is the use of the solar collectors as the energy source, and then it is preferable to warm up the solar collectors by recirculation rather than by storing hot water in the tanks. This preference has been translated in placing greater weights on the use of M8 rather than of M9. These weights are fixed but, in order to make a compromise between gas saving and energy accumulation, if *PSI* does not balance the environmental losses in the collectors (estimated to be equal to $0.464(T_{sco} - T_{amb})$), then the above weights are diminished significantly, hence inverting the priority order between M8 and M9[2]. This strategy avoids that the water in the tanks cools down the collectors making them unusable for a long period and, at the same time, maximizes the ratio between stored energy and auxiliary energy consumption. In fact, M8 is activated when the irradiation is too low for increasing the temperature of the collectors.

[2]Once the accumulation process has started, it yields to the dynamics reported in Eq. 4.

The abstract process description (operating modes), the operating constraints, and the terms entering the cost function are encoded in a HYSDEL model [16], to get a corresponding mixed logical dynamical (MLD) model [4]. A hybrid MPC problem is setup with prediction horizon $N = 1$. The reason for such a short horizon is twofold: first, the continuous dynamics of the process are completely neglected in the abstract hybrid model (one-step buffers are the only states of the hybrid model); second, the mixed-integer inequalities contained in the MLD model define a static set of constraints that, being included in the mixed-integer quadratic programming problem associated with MPC to be solved at the current time step, makes the control action respect all operating (hard and soft) constraints. Note that hybrid MPC with horizon $N = 1$ is often used in several applications, especially in the automotive domain [8, 9].

4. Experimental Results

The multi-layer control setup described in the previous section was first tested in simulation on a detailed Simulink model of the process obtained from the University of Seville, Spain. This investigation was done especially to evaluate the computational complexity of the controller; a performance assessment from the simulation results is not very meaningful, as there is a substantial discrepancy between the simulation model and the real process. Simulations over a time period of 24 hours of process operation were run on a laptop PC 1.86 GHz running Matlab 7.0 and the MIQP solver Cplex 9.1. The resulting CPU time is depicted in Fig. 4: the average CPU time was 4.7 ms, the max CPU time 37.9 ms. Both times are way below the sampling time 10 s of the process.

The multi-layer control architecture was tested on September 22, 2007 on the process in Seville. The Hybrid Toolbox for Matlab and the MIQP solver were interfaced to the process through the OPC Toolbox for Matlab [15], so that the same controller used in simulation can be directly tested on the plant. The resulting experimental results are shown in Figs. 5, 6. Fig. 5 depicts the operating modes chosen by the controller, the output temperature of the tanks during the operation, and the environmental conditions (external temperature and measured solar irradiation per surface unit). The solar power *PSI* mentioned in the previous sections is calculated by multiplying the measure of irradiation coming from the sensors by the surface area of the solar collectors (in this case $39.78m^2$).

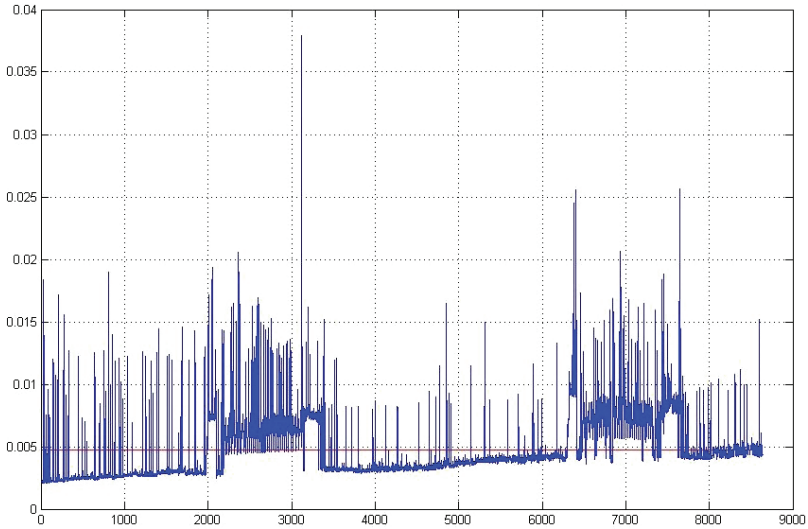

Fig. 4. CPU time (s) measured on a simulation of 24 hours of process operation (8640 sampling steps)

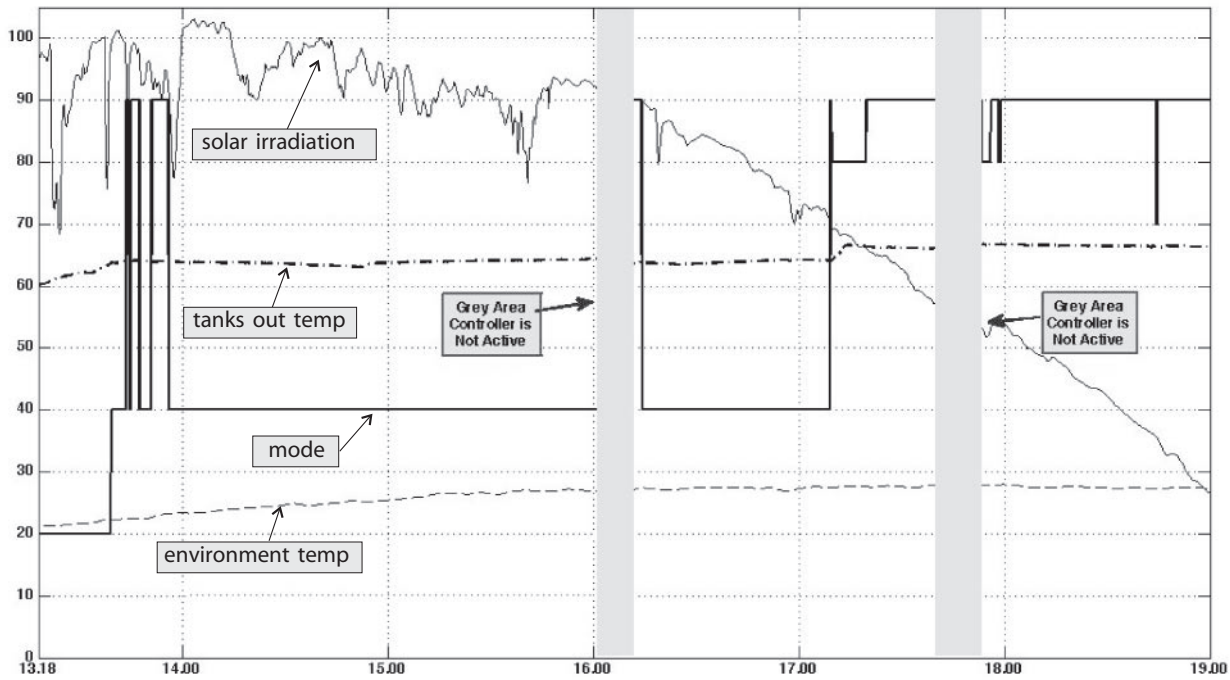

Fig. 5. Experimental results (temperatures are in °C, solar irradiation in W/m^2, mode number is multiplied by 10)

Fig. 6 shows the most significant output trajectories, together with the controlled output of the evaporator and the governed input of the generator. Gray areas represent time intervals in which the process is in open loop (the controller is disabled). In this case the binary and continuous inputs are manoeuvered manually to perturb the system out of his stable region, thus evidencing the time response and the stabilizing effect of the controller in different situations. In the first gray area mode M7 is used to cool down the generator by only using the water coming from the tanks to feed the cooler. Since in this case the tanks temperature is very low (less than 70 °C) the cooler stops working with a consequent (but delayed) loss of the set-point on the output refrigerated temperature. In the following gray area, a malfunction of

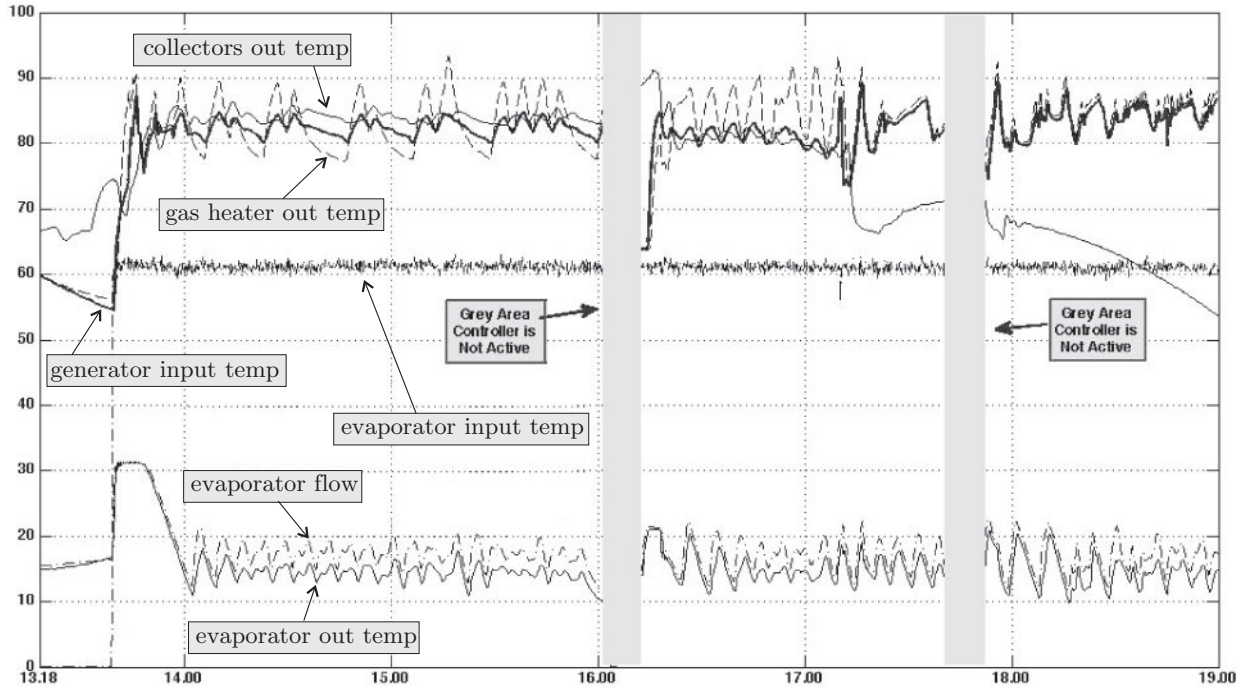

Fig. 6. Experimental results, showing controlled variables related to collectors, evaporator, generator, and gas heater (temperatures are in °C, flows in $\frac{L}{h}/100$)

the system is simulated by forcing the use of solar collectors with a low temperature until the temperature of the input to the generator (and gas heater output) falls below 75 °C. In both cases the response of the controller is satisfactory. Thresholds offsets δ used for this experiments are reported in Appendix A, Table 6.

The controller was activated at 13:18 after the system was manually set in recirculation mode to increase the temperature of solar collectors. In the day of the experiment the weather conditions were rather clouded, as evidenced by the irradiation trajectory. A thermal load simulator is used to impose controlled conditions in the closed-loop system.

Since initially there is no cooling request from the user the control system switches directly to mode M2, storing the energy surplus of the collectors in the tanks. At 13:40 the user requests refrigeration by opening the evaporator circuit and letting water to flow through it. After the evaporator flow gets larger ($> 5000l/h$), the controller automatically switches to a mode that performs cooling, in this case M4 since the output collector temperature is greater than the one of the gas heater. In order to speed up the settling time of the generator input temperature to the set point the mode configuration switches between M4 and M9 until the output temperature of the gas heater reaches a safety value. Afterward, the mode remains in M4, combining use of gas heater with use of solar collectors. This configuration is held until the first disconnection of the controller occurs (gray area). Although the controller never recurs to mode M3 (gas heater valve closed), one can notice that the heater is not always active (burner on) while in mode M4. In mode M4, in fact, working with a low flow ($< 1500l/h$) in the gas heater together with the gas burner off is permitted. This can be seen by looking at the output temperature of the gas heater. In fact, when the gas burner is active the output temperature must oscillate between 84 and 90 °C due to a inner relay but, during M4, T_{GHO} reaches cyclically a minimum value of 78 °C. If PSI keeps a high average value during the use of the collectors, by letting T_{SCO} increasing when mixing with gas fired water, the controller switches to mode M3. The use of solar collectors only is hardly linked to solar irradiation power and the chosen threshold values.

After the first gray area, the controller is activated in an emergency situation, as the input temperature of the generator is out of the allowed range, the cooler is inactive, and the inner temperature of the gas heater is low. The solar output temperature is instead rather high due to forced recirculation. In this case the controller never uses M3, but resorts to M4. This is due to

the fact that the controller keeps into account a variable loose factor $L_{sc,am}$ between solar collectors and absorption machine (the cooler). The subsequent fall of T_{SCO} validates the solution adopted.

We can see that the use of M4 after the first gray area is quite different with respect to the previous case. This depends on the decay of solar irradiation that translates into a more intense use of gas heater. Then, when solar radiation starts becoming insufficient to warm up solar collectors, mode M8 is activated, allowing the storage of energy, even while the refrigeration process is still active. Accumulation in the tanks is performed until T_{SCO} falls below the output temperature of the tanks. In this case the controller switches to M9 in order to avoid losses of tank energy and, at the same time, trying to increase the temperature of collectors at much as possible.

The controller is then disconnected again (next gray area) in order to test its robustness against faults and disturbances when working with only the gas heater to feed the cooler. In this case, when the controller becomes active again, the settling time is slightly larger and presents more oscillations with respect to the recovery after the first disconnection (first gray area). Such an increased settling time is mainly due to the smaller flow circulating in the generator during modes M8/M9 with respect to M4.

Meanwhile the controller is turned off during the second gray area, a new rule was added in the controller: Mode M7 must be executed for a time interval of 10 seconds every half an hour if the output $T_{E,O}$ is in the proper operating range. This new rule serves mainly to verify that the output temperature of tanks to absorption machine is correct. Mode M7 is then executed at 18:45, with no significant changes in the output temperature from the tanks to the cooler.

5. Conclusions

In this paper we have described a multi-layer hybrid control design approach for a rather complex solar air conditioning plant. The proposed control approach is versatile in that it allows one to embed several constraints and heuristic rules in a mixed-integer programming formulation. Compared to approaches where fixed rules are given, on-line optimization leaves more degrees of freedom in selecting the best mode among one or more possible choices that are feasible for the current plant conditions.

The closed-loop results completely satisfy the requested specifications [19]. The results are comparable to those obtained through other alternative control approaches, such as the one described in [7]. The control design described in our paper is able to stabilize the process and is robust against disturbances in solar irradiation and (induced) malfunctioning in the process. For this type of systems it may be interesting to adaptively change the parameters of the controller, to adjust to changing environmental conditions. We believe that the control paradigm described in this paper is easily predisposed for on-line changes of the parameters. In particular, the closed-loop behavior depends on the threshold values of δ defined in Table 6. Future works will investigate ways to update the δ parameters according to the environmental conditions while preserving closed-loop stability and robustness.

Acknowledgments

The authors thank Tomás Fernández for his invaluable help in carrying on the experiments on the plant. This work was supported by the European Commission under the HYCON Network of Excellence, contract number FP6-IST-511368, and by the Italian Ministry for University and Research (MIUR) under project ''Advanced control methodologies for hybrid dynamical systems'' (PRIN'2005).

References

1. Antsaklis PJ. A brief introduction to the theory and applications of hybrid systems. *Proc IEEE Special Issue on Hybrid Systems: Theory and Applications* 2000; 88(7): 879–886.
2. Bemporad A. *Hybrid Toolbox—User's Guide*. January 2004. http://www.dii.unisi.it/ hybrid/toolbox.
3. Bemporad A, Mignone D. *MIQP.M: A Matlab function for solving mixed integer quadratic programs*, 2000. http://www.dii.unisi.it/ ~ hybrid/tools/miqp.
4. Bemporad A, Morari M. Control of systems integrating logic, dynamics, and constraints. *Automatica* 1999; 35(3): 407–427.
5. Branicky MS. *Studies in Hybrid Systems: Modeling, Analysis, and Control*. PhD thesis, LIDS-TH 2304, Massachusetts Institute of Technology, Cambridge, MA, 1995.
6. Camacho E, Berenguel M, Rubio F. *Advanced Control of Solar Plants*. Springer (London), 1997.
7. Ding H, Sonntag C, Engell S, Stursberg O. Hybrid supervisory control of a solar air conditioning plant. In *European Control Conference*, pp 5516–5521, Kos, Greece, 2007.
8. Giorgetti N, Bemporad A, Tseng HE, Hrovat D. Hybrid model predictive control application towards optimal semi-active suspension. In *Proceedings of IEEE International Symposium on Industrial Electronics*, pp 391–398, Dubrovnik, Croatia, 2005.

9. Giorgetti N, Ripaccioli G, Bemporad A, Kolmanovsky IV, Hrovat D. Hybrid model predictive control of direct injection stratified charge engines. *IEEE/ASME Trans Mechatronics* 2006; 11(5): 499–506.
10. Hooker JN, Osorio MA. Mixed logical/linear programming. *Discrete Appl Math* 1999; 96–97: 395–442.
11. ILOG, Inc. *CPLEX 11.0 User Manual*. Gentilly Cedex, France, 2008.
12. Makhorin A. *GLPK (GNU Linear Programming Kit) User's Guide*, 2004.
13. Nunez-Reyez A, Normey-Rico JE, Bordons C, Camacho EF. A Smith predictive based MPC in solar air conditioning plant. *J Process Control* 2005; 15: 1–10.
14. Sayigh AAM (ed). *Solar Air Conditioning and Refrigeration*. Pergamon Press (USA), 1992.
15. The Mathworks, Inc. *OPC Toolbox User's Guide*, 2008.
16. Torrisi FD, Bemporad A. HYSDEL—A tool for generating computational hybrid models. *IEEE Trans Control Syst Technol* 2004; 12(2): 235–249.
17. Tyler ML, Morari M. Propositional logic in control and monitoring problems. *Automatica* 1999; 35(4): 565–582.
18. Williams HP. *Model Building in Mathematical Programming*, 3rd edn. Wiley & Sons, 1993.
19. Zambrano D, Bordons C, Garcıa-Gabın W, Camacho EF. A solar cooling plant: a benchmark for hybrid systems control. In 2nd IFAC Conference on Analysis and Design of Hybrid Systems, pp. 199–204, Alghero, Italy, 2006.
20. Zambrano D, Garcıa-Gabın W, Camacho EF. A heuristic predictive logic controller applied to hybrid solar air conditioning plant. In Bemporad A, Bicchi A, Buttazzo G, editors. *Hybrid Systems: Computation and Control*, vol. 4416 of *Lecture Notes in Computer Science*, pp. 783–786. Springer-Verlag, 2007.

Appendix

Threshold temperatures are not considered here as absolute values but as offsets added to the reference temperature of the generator. The values for the δ_i variables used in equations (5), (6), (7) are given in the Table 6. These thresholds affect the closed-loop performance and have been determined experimentally.